A seven-sex species recognizes self and non-self mating-type via a novel protein complex

Guanxiong Yan[1], Yang Ma[1], Yanfang Wang[2], Jing Zhang[1], Haoming Cheng[1, 3], Fanjie Tan[2], Su Wang[1, 3], Delin Zhang[2], Jie Xiong[1], Ping Yin[2]*, Wei Miao[1, 3, 4, 5]*

[1] Institute of Hydrobiology, Chinese Academy of Sciences, Wuhan 430072, China

[2] National Key Laboratory of Crop Genetic Improvement, Hubei Hongshan Laboratory, Huazhong Agricultural University, Wuhan 430070, China

[3] University of Chinese Academy of Sciences, Beijing 100049, China

[4] State Key Laboratory of Freshwater Ecology and Biotechnology of China, Wuhan 430072, China

[5] CAS Center for Excellence in Animal Evolution and Genetics, Kunming 650223, China

Corresponding author: Wei Miao, miaowei@ihb.ac.cn.

Ping Yin, yinping@mail.hzau.edu.cn.

Abstract

Although most species have two sexes, multisexual species (i.e., those with multiple mating types) are also widespread. However, it is unclear how mating-type recognition is achieved at the molecular level in multisexual species. The unicellular ciliate *Tetrahymena thermophila* has seven mating types, which are determined by the MTA and MTB proteins. In this study, we found that both proteins are essential for cells to send or receive complete mating-type information, and transmission of the mating-type signal requires both proteins to be expressed in the same cell. We found that MTA and MTB form a mating-type recognition complex that localizes to the plasma membrane, but not to the cilia. Stimulation experiments showed that the mating-type-specific regions of MTA and MTB mediate both self- and non-self-recognition, indicating that *T. thermophila* uses a dual approach to achieve mating-type recognition. Our results suggest that MTA and MTB form an elaborate multifunctional protein complex that can identify cells of both self and non-self mating types in order to inhibit or activate mating, respectively.

Impact statement

A giant multifunctional protein complex mediates mating-type recognition through a non-ligand-receptor mechanism in a multisexual species.

Introduction

Sexual reproduction is almost universal among eukaryotic organisms. Mating type (or sex) is a key regulatory feature of gamete fusion. Most species have only two mating types (e.g., male and female, + and -, or a and α) and species usually use either self- or non-self-recognition mechanism to achieve mating-type recognition (Goodenough & Heitman, 2014). However, species in some lineages, such as some ciliates and basidiomycetes (Heitman, 2015; Phadke & Zufall, 2010), possess multiple mating types, and multiple-alleles self-incompatibility system were observed in some plants, such as Brassicaceae (Iwano & Takayama, 2012; Takayama & Isogai, 2005; Vekemans & Castric, 2021). This raises the interesting question of how mating types are recognized at the molecular level in multiple mating-type systems.

The model unicellular ciliate, *Tetrahymena thermophila*, has seven mating types (I–VII). Under starvation conditions, any cell of one mating type can mate with a cell of any of the other six mating types, but not with one of the same mating type (Figure 1A, Figure 1–figure supplement 1, Video 1–3) (Cervantes et al., 2013; Nanney, 1953; Orias et al., 2017; Yan et al., 2021). Mating-type recognition in *Tetrahymena* depends on direct cell–cell contact, which suggests that mating-type proteins localize to the cell surface. However, there is no direct evidence to indicate whether they are ciliary proteins or not. When one cell comes into contact with a cell of a different mating type, a mating-type-dependent recognition event enables both cells to enter a pre-conjugation stage (called costimulation) (Bruns & Palestine, 1975; Finley & Bruns, 1980). Even when cells of different mating types are mixed in unequal ratios (for example, 9 : 1), all cells become fully stimulated (Bruns & Palestine, 1975). Processes that take place

during costimulation include Tip transformation (Wolfe & Grimes, 1979) and concanavalin A (Con-A) receptor appearance (Figure 1B) (Wolfe & Feng, 1988; Wolfe et al., 1986). In preparation for pairing, costimulated cells of the same and different mating type(s) adhere to form very loose pairs. Heterotypic cell pairs form a stable conjugation junction, whereas homotypic pairs separate very quickly (Video 2 and 3) (Kitamura et al., 1986).

The mating-type system of *T. thermophila* was described by Nanney and collaborators in the early 1950s (reviewed in (Orias, 1981; Orias et al., 2017)). We previously showed that mating type is determined by a pair of mating-type genes that are organized in head-to-head orientation: *MTA* and *MTB* (Figure 1C) (Cervantes et al., 2013). Each gene has a terminal exon that encodes five transmembrane (TM) helices and a cysteine-rich growth factor receptor (GFR) domain. The region between the two terminal exons of the gene pair encodes the N-terminal mating-type-specific extracellular regions. Based on the mating-type-specific regions, the mating-type genes are called *MTA1-MTB1* for Mating type I, *MTA2-MTB2* for Mating type II and so on. We previously showed that Δ*MTB* cells do not form pairs or produce progeny and that Δ*MTA* cells retain mating-type specificity but pair extremely poorly and rarely produced progeny (Cervantes et al., 2013); we concluded that the two genes are non-redundant and both are essential for mating. However, challenges such as multiple mating types; the high molecular weight, membrane localization and extremely low expression levels of mating-type proteins; and difficulty in genetically manipulating the mating-type gene locus have so far prevented elucidation of the mode of action of the MTA and MTB proteins and of whether they mediate self- or non-self mating-type recognition.

In this study, we provide direct evidence that the MTA and MTB form an elaborate multifunctional protein complex that can identify cells of both self and non-self mating types to inhibit or activate mating, respectively.

Results

Mating-type recognition cannot be explained by a simple receptor–ligand model

Receptor–ligand interactions are a critical mechanism for intercellular communication that may regulate mating-type recognition in *T. thermophila*, irrespective of whether self- or non-self-recognition mechanisms are employed. Therefore, we first assessed whether mating-type recognition conforms to a straightforward receptor–ligand model (in which one mating-type protein acts as the receptor and the other as the ligand) and whether self or non-self is recognized (Figure 2–figure supplement 1A, 1 and 2). For this, we determined whether deletion of each mating-type gene affected the transmission and detection of mating signals to and from wild-type (WT) cells (Figure 2A shows the experimental procedure) by assessing the ability of cells to undergo costimulation (the prerequisite for mating). Our experiment allows us to test if cells missing one of the two mating-type proteins can still costimulate WT cells (Figure 2–figure supplement 1A, 3 and 6).

In *T. thermophila*, cells normally enter into the fully costimulation stage within ~30 min after mixing starved WT cells of two different mating types, and start pair formation during the next ~30 min (Figure 2B, black line). Cells that have already been costimulated immediately start forming pairs with other costimulated cells of a different mating type (Figure 2B, red line).

To our surprise, the rate of pair formation in WT cells pre-incubated with either Δ*MTA* cells (Figure 2B, green line) or Δ*MTB* cells (Figure 2B, blue line) did not increase (i.e., costimulation did not occur). These results were not changed by extending the pre-incubation time (Figure 2–figure supplement 1B). Therefore, both MTA and MTB proteins are essential for the mating-type signal; there is no simple receptor–ligand relationship.

In addition, WT cells were not costimulated even when they were simultaneously incubated with both Δ*MTA* and Δ*MTB* cells (Figure 2B, teal line), although, according to the receptor–ligand model, they should have received "MTA stimulation" from Δ*MTB* cells and "MTB stimulation" from Δ*MTA* cells. This result indicates that the absence of a mating-type protein in one cell cannot be complemented by its presence in another cell in the same culture; the MTA and MTB proteins must be in the same cell to transmit the mating-type signal. This finding suggests that mating-type recognition cannot be explained by a simple receptor–ligand model. It is possible that the MTA and MTB proteins form a complex which either serves as a recognizer (functioning as both ligand and receptor) or a co-receptor (which influences ligand–receptor activity). But, since MTA and MTB are the only genes with mating-type-specificity, it is unlikely that the complex is acting as a co-receptor.

Mating-type proteins differentially regulate two steps of costimulation

During costimulation, cells undergo a sequence of developmental events that remodel the anterior cell membrane and its associated cytoskeleton (Cole, 2013). Two hallmarks of this process are Tip transformation (in which the anterior tip of the cell becomes curved) and Con-A

117 receptor appearance (receptors bound by the plant lectin concanavalin A, which binds to
118 mannose containing glycoproteins). When WT cells of one mating type were mixed with WT cells
119 of another mating type, the cell tips became transformed (Figure 2C, 5 and 9) and Con-A
120 receptors appeared in almost all cells (Figure 2D, 4). When WT cells were pre-incubated with
121 Δ*MTA*, Δ*MTB*, or both cell types, Tip transformation was not observed in any cell (Figure 2C, 6–
122 8). Similarly, when cells of each mutant were pre-incubated with WT cells, Tip transformation
123 was not detected (Figure 2C, 10 and 11). The outcome was slightly different for Con-A receptor
124 appearance. Con-A receptors were not observed in WT cells pre-incubated with Δ*MTB* cells
125 (Figure 2D, 6) or in cells of either mutant pre-incubated with WT cells (Figure 2D, 7 and 8). In
126 contrast, when WT cells were exposed to Δ*MTA* or "Δ*MTA* cells plus Δ*MTB* cells", the Con-A
127 receptor was detected (Figure 2D, 5 and 9); this is consistent with Δ*MTA* cells retaining a very
128 weak ability to pair (Cervantes et al., 2013). These results indicate that neither Δ*MTA* and Δ*MTB*
129 cells can fully stimulate WT cells or be stimulated by WT cells. They also demonstrate that
130 costimulation can be separated into two stages: (i) the appearance of Con-A receptors, which
131 requires the expression of MTB only in partner cells, and (ii) morphological transformation of the
132 cell tip, which requires both MTA and MTB.

133 **Mating-type proteins form a complex with several coexpressed proteins**

134 The inability of "Δ*MTA* cells plus Δ*MTB* cells" to costimulate WT cells of a different mating
135 type indicates that MTA and MTB proteins can only function when expressed on the same cell
136 (Figure 2B, teal; Figure 2C, 8). We previously found that CDK19 and CYC9 proteins are also

137 essential for mating. Δ*CDK19* and Δ*CYC9* cells cannot mate with other cells, but they still express
138 MTA and MTB proteins (Ma et al., 2020). In WT cells, the pairing rate was increased following
139 pre-incubation with Δ*CDK19* or Δ*CYC9* cells of a different mating type (Ma et al., 2020). These
140 results further support the idea that MTA and MTB must be expressed on the same cell to be
141 fully functional, leading us to hypothesize that MTA and MTB proteins form a mating-type
142 recognition complex (MTRC).

143 To test whether MTA and MTB proteins physically interact, an HA-tag coding sequence was
144 ligated to the 3' end of the *MTA* gene (Figure 3A); cellular proteins were co-precipitated with HA-
145 tagged MTA and analyzed by immunoprecipitation-coupled mass spectrometry (IP-MS). As
146 expected, the MTB protein co-purified with MTA (Figure 3B, C), as did another set of proteins,
147 which we named MRC1–MRC6 (Figure 3B, C and Figure 3–Source data 1 and 2). Next, we
148 produced strains expressing either HA-tagged MTB or MRC1 (Figure 3A), and found that each
149 protein pulled down a subset of the proteins that co-purified with MTA (Figure 3B, C).
150 Unfortunately, these pull-down experiments were not as successful as the MTA IPs, perhaps
151 because of the higher molecular weight of MTB and MRC1. Taken together, our results suggest
152 that MTA, MTB, and MRC1–MRC6 form the MTRC. Alternatively, MTA and MTB may interact with
153 subsets of MRC proteins to form smaller complexes or alternative MTRCs. Different protein
154 interactors were identified in extracts from cells at different mating stages. This may reflect
155 conformational changes in the MTRC but the huge molecular weight of the complex and
156 extremely low expression levels of its proteins make this possibility difficult to investigate.

Mating-type-related factors in other species are often relatively small (Iwano & Takayama, 2012; Kahmann & Bölker, 1996), but those of *T. thermophila* are large proteins (predicted size, 92–212 kDa). Figure 3D shows the predicted domains of the MRC1–MRC6 proteins. Like MTA and MTB, MRC1 has five predicted TM helices and a GFR domain. MRC2 has eight TM helices and a pectin lyase-fold domain, suggesting a possible role in carbohydrate chain modification. MRC3 has two TM helices in the central region and an adjacent ~35 amino acid (aa) poly-E region. MRC4 and MRC5 (previously named TPA9 (Wang et al., 1997; Wang & Takeyasu, 1997)) are both P-type ATPases that are likely to function as calcium-translocators. MRC6 has four TM helices and a P-loop containing nucleoside triphosphate hydrolases. Most of the MRC genes are highly coexpressed with *MTA* and *MTB* (Figure 3E). Examination of the whole genome sequences of strains with mating types II–VII (Wang et al., 2020), confirmed that only the sequences of *MTA* and *MTB* genes are mating-type-specific.

In addition to the MRC proteins, CDK19, CYC9, CIP1, and AKM3 were identified in IP-MS experiments, but with relatively few supporting peptides (Figure 3C). Our previous work showed that CDK19, CYC9, and CIP1 are components of a cyclin-dependent kinase complex. These genes are coexpressed with *MTA* and *MTB* (Figure 3E) and are important for mating, and the encoded proteins localize to the cell tip and pairing junction (Ma et al., 2020). AKM3 is predicted to be a K^+ channel of unknown biological function. It is coexpressed with *MTA* and *MTB* (Figure 3E), and we found that the *AKM3* deletion strain cannot pair. Therefore, these four proteins are also likely to interact with the mating-type proteins (perhaps indirectly and/or via weak interactions) and might be involved in downstream signaling following mating-type recognition.

Mating-type proteins localize to the cell surface but not to the cilia

We used the MTA7-HA strain to determine the localization of mating-type proteins. Cell fractionation (Figure 4–figure supplement 1) revealed that MTA7-HA is a membrane protein (Figure 4A). Biotinylation and isolation of cell surface proteins confirmed that MTA7-HA is exposed on the cell surface (Figure 4B). To investigate whether MTA7-HA localizes to the cilia membrane, we isolated and collected cilia (Figure 4C) and then analyzed cilia protein extracts by IP-coupled western blotting (WB) and MS. MS analysis identified typical ciliary proteins, such as inner and outer arm dynein proteins (Figure 4–Source data 1). However, both IP-WB (Figure 4D) and MS (Figure 4–Source data 1) consistently failed to identify MTA7-HA protein in the cilia fraction. These results conclusively indicate that MTA7-HA localizes to the cell surface, but not to cilia. Unfortunately, we failed to detect MTA7-HA by immunofluorescence staining of cells at any mating stage (starvation, costimulation, or conjugation), probably due to the epitope masking and extremely low expression level.

To further examine localization of the mating-type proteins, eGFP-tagged MTB2 was overexpressed from an exogenous locus (Figure 4E). This strain (which has a mating type VI background) mated normally with WT cells of all mating types except for VI and II. This result indicates the overexpressed MTB2-eGFP protein is fully functional for mating. Interestingly, cells of this strain can also mate with one another (self-mating); a similar phenotype was previously reported for strains expressing multiple mating-type proteins (Lin & Yao, 2020). The overexpressed MTB2-eGFP protein was detected on the cell surface in a linear pattern radiating from the cell tip to the cell body along the ciliary rows (Figure 4F, costimulated cell; Figure 4G,

mating pair), although signals are also apparent between ciliary rows. Co-staining with a tubulin dye showed that the MTB2-eGFP protein is adjacent to, rather than co-localizing with, the base of cilia (Figure 4F, G, enlarged). Confocal images from the interior of the cell and through the cilia showed that MTB2-eGFP localizes to the cell surface (and also to intracellular structures, probably the endoplasmic reticulum (ER) and Golgi), but not to the cilia (Figure 4–figure supplement 2), confirming our results with the MTA7-HA protein (Figure 4A-D). MS analysis showed that overexpressed MTB2-eGFP protein was not present in isolated cilia of the *MTB2-eGFP* strain (Figure 4–Source data 2). Therefore, mating-type proteins localize to the cell surface, as might be expected since mating-type recognition depends on cell–cell contact.

Mating-type proteins influence non-self-recognition

The mating-type-specific region of the *MTA* and *MTB* gene pair is the only known genetic locus with mating-type specificity; therefore, we next tested whether this region influences self- and/or non-self mating-type recognition. For this, we expressed the extracellular region of MTA (MTAxc) or MTB (MTBxc) in an insect cell secreted expression system, purified the recombinant proteins (Figure 5–figure supplement 1), and then tested their effect on mating behavior.

First, we tested whether MTAxc and MTBxc can influence mating in cells with a different mating-type specificity (i.e., non-self-recognition). When WT cells were incubated with MTAxc (and/or MTBxc) of a different mating type, markers of costimulation were not observed (Figure 5–figure supplement 2). Surprisingly, treated cells had a significantly increased pairing rate. Compared with controls (Figure 5A–C, black), WT cells (VI and VII) pre-treated with MTAxc or MTBxc of different mating types (VII and VI, respectively) had an increased pairing rate

(Figure 5A–C, green or blue), with a stronger effect after pre-treatment with both MTAxc and MTBxc (Figure 5A–C, teal). Dose–effect assays showed that pairing rates increased with increasing MTA6xc and MTB6xc concentrations between 3 pg/ml and 30 pg/ml, with the effect becoming saturated or weaker at higher concentrations (Figure 6A–F). MTAxc and MTBxc also stimulated mating for all other WT mating types (Figure 6G, H), indicating that this is a general effect. Based on these results, we conclude that the mating-type-specific regions of MTA and MTB proteins are involved in non-self mating-type recognition.

Mating-type proteins also influence self-recognition

We used similar methods to examine whether pre-treatment with a cognate mating-type-specific region (i.e., self-recognition) affects mating. Treatment of WT cells (VI and VII) with MTAxc and/or MTBxc of the same mating type decreased the pairing rate (Figure 5D, E, green or blue). No obvious difference was found between treatments with either MTAxc or MTBxc. Meanwhile, a significant synergistic effect was observed (Figure 5D, E, teal). For all treatments (single or combined), the pairing rate was similar by 4 h (reaching >80%; Figure 5D, F), indicating that the initial inhibitory effect on pairing was eventually overcome. Negative regulation by MTAxc and MTBxc was also observed for other mating-type combinations (Figure 6I, J). These results support the idea that the mating-type-specific regions of MTA and MTB proteins mediate both non-self (between cells of different mating types) and self (between cells of same mating type) recognition.

Discussion

Although the basic biological features of the *T. thermophila* mating-type system were discovered over half a century ago, the mechanism for mating-type recognition remains unclear. Here, we identified a novel MTRC that contains MTA, MTB, and several other proteins and provide evidence that MTA and MTB mediate both self and non-self mating-type recognition.

In most species, mating signals are associated with relatively small proteins or molecules (Iwano & Takayama, 2012; Kahmann & Bölker, 1996). However, in *T. thermophila*, the MTRC is likely to be over a million Daltons in size. This large size is consistent with its multiple functions: An elaborate MTRC is needed to inhibit mating between cells of the same mating type while also activating mating between cells of different mating types. This is likely to be a highly complex process, given that there are seven mating types in all. Further structural studies of this protein complex may reveal the specific self- and non-self-recognition mechanisms.

An open question is why *T. thermophila* should use such a dual approach to achieving mating-type recognition. Recent research on basidiomycetes and flowering plants (other species with multiple mating types) has shown that their mating-type recognition (or self-incompatibility) mechanisms involve either self- or non-self-recognition (Fraser & Heitman, 2003; Iwano & Takayama, 2012; Vekemans & Castric, 2021). Our previous evolutionary study showed that the length of the mating-type-specific region differs significantly among different *Tetrahymena* species (Yan et al., 2021). Based on the massive difference in length, it is reasonable to speculate that different species might use different mechanisms for mating-type recognition. Therefore, dramatic evolution of the mating-type recognition mechanism seems to

have occurred relatively soon after the emergence of the *Tetrahymena* genus. Further detailed functional and evolutionary studies may reveal how and why this recognition mechanism evolved and how its evolution contributed to speciation.

We still do not know what intracellular signals are transduced when the MTRCs on two cells interact. Mating-type self-recognition might generate an inhibitory signal or might simply inactivate the MTRC. In many species, such as *Papaver rhoeas* and *Ciona intestinalis*, interaction between mating-type proteins of the same mating type induces changes in cytoplasmic Ca^{2+} concentration that cause self-incompatibility (Giamarchi et al., 2006; Harada et al., 2008; Wu et al., 2011). A similar system may exist in *T. thermophila*, since the MRC4 and MRC5 proteins are predicted to be Ca^{2+}-translocators. Interaction between MTRCs on cells of different mating types (non-self-recognition) should result in their activation to allow the cells to initiate pairing. We propose that the activation signal involves the CDK19 complex (a cyclin-dependent kinase complex) (Ma et al., 2020) and AKM3 (a K^+ channel; Figure 3C) because they probably interact with the MTRC. We expect future studies to lead to the discovery of more detailed mechanisms for mating-type recognition and initiation of conjugation involving these proteins.

Paramecium tetraurelia, a closely related Oligohymenophorean ciliate, has only two mating types, which are determined by the expression or non-expression of a *Tetrahymena*-MTA/B-like protein called mtA (Singh et al., 2014; Yan et al., 2021). An intriguing question is whether mtA also engages in the formation of a MTRC with other proteins by serving as a recognizer rather than mediating a straightforward receptor–ligand interaction. Future investigations of *Paramecium tetraurelia* may shed light on the origins and evolutionary aspects of this distinctive

mating system. Moreover, due to the extremely long evolutionary distance, recognition mechanisms discovered in model species fall short of explaining many of the intricate biological events in protists. Insight into the detailed function of MTRC could contribute to our understanding of cell–cell recognition processes in other species, such as *Toxoplasma* and *Plasmodium*.

Materials and Methods

Biological methods

Strains used in this study are summarized in Appendix 1–table 1. All cell growth, starvation, and pairing experiments were conducted at 30°C. Cells were grown in Super Proteose Peptone (SPP) medium (1% Proteose Peptone, 0.1% yeast extract, 0.2% glucose, 0.003% Sequestrene) or Neff medium (0.25% Proteose Peptone, 0.25% yeast extract, 0.5% glucose, 0.003% Sequestrene). Cells were starved in 10 mM Tris-Cl (pH 7.4) for ~16 h before all pairing experiments. For normal pairing assays, equal numbers of starved cells of different mating types (at ~2×10^6 cells/ml) were mixed. To obtain costimulated (pre-incubated) cells, two starved strains were mixed at a 9 : 1 ratio for ~30 min (unless otherwise stated). Before mixing costimulated cells, any potentially pairing cells were separated by shaking. Figure 2A shows the setup of costimulation experiments. For all mating experiments (whether or not they involved mutant cells), the starting WT cell density was ~2×10^6 cells/ml. The following formula was used to calculate pairing ratios and correct for the presence of mutant cells:

$$\%cells\ paired = \frac{2 \times \#\ pairs}{(2 \times \#\ pairs + \#\ unpaired\ cells) \times \%\ WT\ cells} \times 100$$

Somatic gene deletion, truncation, and protein tagging

To construct deletion strains, a ~1 kb fragment upstream of the gene's open reading frame (ORF) (#1), a ~0.5 kb fragment downstream of the gene's ORF (#2), and a ~1 kb fragment downstream of #2 (#3) were amplified. Fragments #2 and #3 were joined to the *NEO4* cassette (Cd^{2+}-inducible *MTT1* promoter linked to the neomycin resistance gene) by fusion PCR and then cloned into the pBlueScript SK (+) vector together with fragment #1. In this way, #1-#2-*NEO4*-#3 constructs were obtained for the next transformation. HA-tagged strains were constructed in a similar way, except that fragment #1 was upstream of the stop codon or upstream of the terminal intron. To obtain the MTB2-eGFP construct, MTB2-coding sequences replaced the MTT1-coding sequence (Figure 4E) and the construct was made using the large DNA fragment assembly method (Jiang et al., 2022). Constructs were introduced into starved WT cells by biolistic transformation to obtain deletion strains (Mochizuki, 2008). Positive clones were selected in SPP medium containing decreasing Cd^{2+} concentrations (from 1 μg/ml to 0.05 μg/ml) and increasing paromomycin concentrations (from 120 μg/ml to 40 mg/ml) until all WT somatic chromosomes had been replaced by mutant ones, as determined by PCR using checking primers. All primers used are listed in Appendix 1–table 2.

Immunoprecipitation and mass spectrometry

The IP method was adapted from a published method (Tian et al., 2017). To pull down HA-tagged proteins from *T. thermophila*, cells were harvested from 500 ml cultures (density ~3×10^6 cells/ml). Cells were then treated for 20 min with paraformaldehyde (PFA) (at a final concentration of 0.3%) to stabilize protein–protein interactions, washed with PB buffer (2.7 mM KCl, 8 mM Na_2HPO_4, 1.5 mM K_2HPO_4), and blocked with 125 mM glycine. Cells were then

323 resuspended in lysis buffer (1% Triton X-100, 30 mM Tris-HCl, 20 mM KCl, 2 mM $MgCl_2$, 1 mM
324 phenylmethylsulfonyl fluoride, 150 mM NaCl, cOmplete proteinase inhibitor [Roche Diagnostics,
325 Indianapolis, IN, USA]), lysed by ultrasonic treatment and incubated with EZview anti-HA agarose
326 beads (Sigma-Aldrich, St Louis, MO, USA) for 2.5 h at 4°C. The beads were washed with wash
327 buffer (1% Triton X-100, 600 mM NaCl, 30 mM Tris-HCl, 20 mM KCl, 2 mM $MgCl_2$, cOmplete
328 proteinase inhibitor) to remove nonspecific-binding proteins and then HA-tagged proteins were
329 eluted with HA peptides (Sigma-Aldrich). WT samples (not HA tagged) were run in parallel for
330 each sample. In total, data for 13 WT controls were combined to identify non-specific binding
331 proteins.

332 For MS, the EASY-nLC chromatography system (Thermo Scientific, Rockford, IL, USA) was
333 coupled on-line to an Orbitrap Elite instrument (Thermo Scientific) via a Nanospray Flex Ion
334 Source (Thermo Scientific). Xtract software (Thermo Scientific) and Proteome Discoverer 2.1
335 software were used for MS data analysis based on a database that combines the 2014 version of
336 whole genome protein annotation (http://ciliate.org/index.php/home/downloads, which
337 contains the whole length sequence of MTA6 and MTB6) and mating-type-specific regions of all
338 other mating-type proteins. IP data were analyzed using CRAPome (Mellacheruvu et al., 2013).

339 **Membrane protein extraction**

340 Figure 4–figure supplement 1A shows the workflow used for membrane protein extraction. Cells
341 were collected, resuspended in 20 ml lysis buffer (150 mM NaCl, 25 mM HEPES, 10% glycerol,
342 2 mM PMSF, 2.6 µg/ml aprotinin, 1.4 µg/ml pepstatin, 10 µg/ml leupeptin, pH 7.4), and lysed by
343 high-pressure homogenization. The lysate was clarified first at low speed (14,000 rpm, 4°C,

15 min), and then at high speed (150,000 g, 4°C, 1 h). The pellet was resuspended in 5 ml lysis buffer containing 1% DDM (Anatrace, Maumee, OH, USA) and rotated for 2 h at 4°C to extract the membrane proteins. Undissolved material was removed by centrifugation (14,000 rpm, 4°C, 30 min). The membrane protein extract was incubated with EZview anti-HA agarose beads for 2.5 h at 4°C and then washed with 5 ml lysis buffer.

Biotinylation and isolation of cell surface proteins

Pierce Cell Surface Protein Biotinylation and Isolation Kit (Thermo Scientific) was used to biotinylate and isolate cell surface proteins. For this, 75 ml cells (density ~3×10^6 cells/ml) were harvested and washed once with BupH phosphate-buffered saline (PBS; 137 mM NaCl, 2.7 mM KCl, 4.3 mM Na_2HPO_4, 1.4 mM KH_2PO_4). Cells were then resuspended in 75 ml PBS containing 0.72 mg/ml Sulfo-NHS-SS-biotin and incubated at room temperature for 10 min. After two washes with 50 ml ice-cold BupH Tris buffer, cells were resuspended in 3 ml lysis buffer (PBS containing 1% Triton X-100, 1 mM phenylmethylsulfonyl fluoride and cOmplete proteinase inhibitor [Roche Diagnostics]), lysed by ultrasonic treatment and incubated with 1.2 ml NeutrAvidin Agarose for 0.5 h at room temperature. The resin was washed four times with 0.5 ml wash buffer and then cell surface proteins were eluted with 1.2 ml elution buffer (with 10 mM DTT). Before WB, cell surface protein samples were concentrated into 0.1 ml volumes using a 30 kDa centrifugal concentrator (Merck Millipore).

Ciliary protein collection

To remove cilia, 500 ml cells (density ~3×10^6 cells/ml) were harvested at room temperature and resuspended in 25 ml 10 mM Tris-Cl (pH 7.4), to which 50 ml medium A (10 mM $EDTA_2Na$,

50 mM sodium acetate, pH 6.0) was added. After 30 s, 25 ml cold distilled water was added; 1 min later, 0.25 ml 0.4 M $CaCl_2$ was added and incubated for 15 s. The cilia were detached from the calcium-shocked cells by vortexing three times for 5 s at 15 s intervals. To collect the cilia, cell bodies were removed by two rounds of centrifugation at 1500 rpm for 5 min at 4°C, and then cilia were collected by centrifugation at 15000 rpm for 15 min at 4°C.

Cytological methods

For tubulin staining, cells were collected and fixed in PHEM buffer (30 mM PIPES, 14 mM HEPES, 5 mM EGTA and 2 mM $MgSO_4$) containing 1% PFA and incubated for 30 min at 4°C. After three washes with PBS (10 min each), Tubulin-Atto 594 was added and incubated for 1 h at 25°C. Finally, cells were washed three times with PBS (10 min each). Fluorescein-labeled Con-A labeling was performed as previously reported (Ma et al., 2020). In brief, cells were fixed and stained with fluorescein-labeled Con-A (Vector Laboratories, Burlingame, CA, USA) at 37.5 μg/ml for 5 min and then washed three times with PB. For analysis of Tip transformation, cells were observed and photographed as soon as possible after fixation with 1% PFA. To distinguish between cell strains in a pairing mixture, starved cells of one strain were labeled with 500 nM MitoTracker (Invitrogen, Eugene, OR, USA), followed by two washes with 10 mM Tris-Cl (pH 7.4) before mixing.

Expression and purification of the extracellular region of mating-type proteins

Coding sequences of the extracellular region of mating-type proteins (MTA6xc, MTB6xc, MTA7xc, and MTB7xc) were codon-optimized and synthesized for expression in an insect-cell system (*Trichoplusia ni* Hi5 cells). Codon-optimized sequences were cloned into pFastBac vectors

containing an N-terminal hemolin signal peptide sequence and a C-terminal 10×His tag sequence. The obtained constructs were transformed into competent DH10Bac cells and individual bacmids were transfected into *Spodoptera frugiperda* Sf9 cells. Recombinant Baculoviruses were collected after 4 days and used to infect *Trichoplusia ni* Hi5 cells for protein expression. Proteins were harvested 60 h after infection and purified with Ni-NTA Superflow resin (Qiagen), anion-exchange chromatography (Source 15Q, GE Healthcare), and size-exclusion chromatography (Superdex-200 Increase 10/300, GE Healthcare).

Bioinformatics analysis

All microarray data were derived from *Tetra*FGD (Xiong et al., 2011) (http://tfgd.ihb.ac.cn/). DNA sequencing data for mating type II–VII cells are derived from a previous report (Wang et al., 2020). Compute pI/Mw (https://web.expasy.org/compute_pi/) was used to predict protein molecular weight. InterProScan (http://www.ebi.ac.uk/interpro/) was used for function and domain annotation (Jones et al., 2014).

Statistical analysis

For mating experiments, more than 100 unpaired cells or cell pairs were counted, with three to five independent replicates. GraphPad software (version 8.0.2) was used for statistical analysis based on ANOVA (matched, Fisher's LSD test).

Acknowledgments

We thank Eduardo Orias (University of California Santa Barbara), Eileen P. Hamilton (University of California Santa Barbara), and Kazufumi Mochizuki (University of Montpellier) for their help and suggestions about experiment design and manuscript writing, and Yunfei Wei (Huazhong

University of Science and Technology) for tubulin staining using Tubulin-Atto 594. We also thank members of the Protist 10,000 Genomes Project (P10K) consortium for helpful suggestions. We would like to thank Min Wang at the Analysis and Testing Center of Institute of Hydrobiology, Chinese Academy of Sciences for her help with mass spectrometry. The bioinformatics analysis was supported by the Wuhan Branch, Supercomputing Center, Chinese Academy of Sciences, China. Culture and maintenance of *Tetrahymena* cells were supported by the National Aquatic Biological Resource Center (NABRC).

Funding information

This work was funded by Bureau of Frontier Sciences and Education, Chinese Academy of Sciences (No. ZDBS-LY-SM026), National Natural Science Foundation of China (No. 32130011, 32200344) and China Postdoctoral Science Foundation (No. 2021M703433).

Author Contributions

G.Y. performed the experiments and analyzed the data. Y.M and H.C helped to construct mutants and perform cellular experiments. Y.W. and F.T. performed protein expression and purification experiments. J.Z helped to maintenance of *Tetrahymena* strains. G.Y. wrote the manuscript. All of the authors helped to conceptualize the work, and edit the text and the figures. W.M. and P.Y. supervised the work.

Conflict of Interest

Authors declare that they have no competing interests.

References

427 Adair, W. S., Barker, R., Turner, R. S., & Wolfe, J. (1978). Demonstration of a cell-free factor involved in
428 cell interactions during mating in *Tetrahymena*. *Nature*, *274*(5666), 54-55.
429 Bruns, P. J., & Palestine, R. F. (1975). Costimulation in *Tetrahymena pyriformis*: A developmental
430 interaction between specially prepared cells. *Developmental Biology*, *42*(1), 75-83.
431 https://doi.org/https://doi.org/10.1016/0012-1606(75)90315-2
432 Cervantes, M. D., Hamilton, E. P., Xiong, J., Lawson, M. J., Yuan, D., Hadjithomas, M., Miao, W., &
433 Orias, E. (2013). Selecting one of several mating types through gene segment joining and
434 deletion in *Tetrahymena thermophila*. *PLOS Biology*, *11*(3), e1001518.
435 https://doi.org/10.1371/journal.pbio.1001518
436 Cole, E. S. (2013). *The Tetrahymena Conjugation Junction. In: Madame Curie Bioscience Database*
437 *[Internet].* Landes Bioscience.
438 Finley, M. J., & Bruns, P. J. (1980). Costimulation in *Tetrahymena* II. A nonspecific response to
439 heterotypic cell-cell interactions. *Developmental Biology*, *79*(1), 81-94.
440 https://doi.org/https://doi.org/10.1016/0012-1606(80)90074-3
441 Fraser, J. A., & Heitman, J. (2003). Fungal mating-type loci. *Current Biology*, *13*(20), R792-795.
442 https://doi.org/10.1016/j.cub.2003.09.046
443 Fujishima, M., Tsuda, M., Mikami, Y., & Shinoda, K. (1993). Costimulation-induced rounding in
444 *Tetrahymena thermophila*: early cell shape transformation induced by sexual cell-to-cell
445 collisions between complementary mating types. *Developmental Biology*, *155*(1), 198-205.
446 https://doi.org/10.1006/dbio.1993.1018
447 Giamarchi, A., Padilla, F., Coste, B., Raoux, M., Crest, M., Honore, E., & Delmas, P. (2006). The versatile
448 nature of the calcium-permeable cation channel TRPP2. *EMBO Reports*, *7*(8), 787-793.
449 https://doi.org/10.1038/sj.embor.7400745
450 Goodenough, U., & Heitman, J. (2014). Origins of eukaryotic sexual reproduction. *Cold Spring Harbor*
451 *Perspectives in Biology*, *6*(3). https://doi.org/10.1101/cshperspect.a016154
452 Harada, Y., Takagaki, Y., Sunagawa, M., Saito, T., Yamada, L., Taniguchi, H., Shoguchi, E., & Sawada, H.
453 (2008). Mechanism of self-sterility in a hermaphroditic chordate. *Science*, *320*(5875), 548-
454 550.
455 Heitman, J. (2015). Evolution of sexual reproduction: a view from the Fungal Kingdom supports an
456 evolutionary epoch with sex before sexes. *Fungal Biology Reviews*, *29*(3-4), 108-117.
457 https://doi.org/10.1016/j.fbr.2015.08.002
458 Iwano, M., & Takayama, S. (2012). Self/non-self discrimination in angiosperm self-incompatibility.
459 *Current Opinion in Plant Biology*, *15*(1), 78-83. https://doi.org/10.1016/j.pbi.2011.09.003
460 Jiang, S., Tang, Y., Xiang, L., Zhu, X., Cai, Z., Li, L., Chen, Y., Chen, P., Feng, Y., Lin, X., Li, G., Sharif, J., &
461 Dai, J. (2022). Efficient de novo assembly and modification of large DNA fragments. *Sci China*
462 *Life Sci*, *65*(7), 1445-1455. https://doi.org/10.1007/s11427-021-2029-0
463 Jones, P., Binns, D., Chang, H. Y., Fraser, M., Li, W., McAnulla, C., McWilliam, H., Maslen, J., Mitchell,
464 A., Nuka, G., Pesseat, S., Quinn, A. F., Sangrador-Vegas, A., Scheremetjew, M., Yong, S. Y.,
465 Lopez, R., & Hunter, S. (2014). InterProScan 5: genome-scale protein function classification.
466 *Bioinformatics*, *30*(9), 1236-1240. https://doi.org/10.1093/bioinformatics/btu031

Kahmann, R., & Bölker, M. (1996). Self/Nonself Recognition in Fungi: Old Mysteries and Simple Solutions. *Cell*, *85*(2), 145-148. https://doi.org/https://doi.org/10.1016/S0092-8674(00)81091-0

Kitamura, A., Sugai, T., & Kitamura, Y. (1986). Homotypic pair formation during conjugation in *Tetrahymena thermophila*. *Journal of Cell Science*, *82*, 223-234.

Lin, I. T., & Yao, M. C. (2020). Selfing mutants link Ku proteins to mating type determination in *Tetrahymena*. *PLOS Biology*, *18*(8), e3000756. https://doi.org/10.1371/journal.pbio.3000756

Ma, Y., Yan, G., Han, X., Zhang, J., Xiong, J., & Miao, W. (2020). Sexual cell cycle initiation is regulated by CDK19 and CYC9 in *Tetrahymena thermophila*. *Journal of Cell Science*, *133*(6). https://doi.org/10.1242/jcs.235721

Mellacheruvu, D., Wright, Z., Couzens, A. L., Lambert, J. P., St-Denis, N. A., Li, T., Miteva, Y. V., Hauri, S., Sardiu, M. E., Low, T. Y., Halim, V. A., Bagshaw, R. D., Hubner, N. C., Al-Hakim, A., Bouchard, A., Faubert, D., Fermin, D., Dunham, W. H., Goudreault, M., . . . Nesvizhskii, A. I. (2013). The CRAPome: a contaminant repository for affinity purification-mass spectrometry data. *Nature methods*, *10*(8), 730-736. https://doi.org/10.1038/nmeth.2557

Mochizuki, K. (2008). High efficiency transformation of *Tetrahymena* using a codon-optimized neomycin resistance gene. *Gene*, *425*(1-2), 79-83. https://doi.org/10.1016/j.gene.2008.08.007

Nanney, D. L. (1953). Nucleo-Cytoplasmic Interaction during Conjugation in *Tetrahymena*. *Biological Bulletin*, *105*(1), 133-148. https://doi.org/10.2307/1538562

Orias, E. (1981). Probable somatic DNA rearrangements in mating type determination in *Tetrahymena thermophila*: A review and a model. *Developmental Genetics*, *2*(2), 185-202. https://doi.org/doi:10.1002/dvg.1020020205

Orias, E., Cervantes, M. D., & Hamilton, E. P. (2011). *Tetrahymena thermophila*, a unicellular eukaryote with separate germline and somatic genomes. *Research in Microbiology*, *162*(6), 578-586. https://doi.org/10.1016/j.resmic.2011.05.001

Orias, E., Singh, D. P., & Meyer, E. (2017). Genetics and Epigenetics of Mating Type Determination in *Paramecium* and *Tetrahymena*. *Annual Review of Microbiology*, *71*(1).

Phadke, S. S., & Zufall, R. A. (2010). Rapid diversification of mating systems in ciliates. *Biological Journal of the Linnean Society*, *98*(1), 187-197.

Singh, D. P., Saudemont, B., Guglielmi, G., Arnaiz, O., Gout, J. F., Prajer, M., Potekhin, A., Przybos, E., Aubusson-Fleury, A., Bhullar, S., Bouhouche, K., Lhuillier-Akakpo, M., Tanty, V., Blugeon, C., Alberti, A., Labadie, K., Aury, J. M., Sperling, L., Duharcourt, S., & Meyer, E. (2014). Genome-defence small RNAs exapted for epigenetic mating-type inheritance. *Nature*, *509*(7501), 447-452. https://doi.org/10.1038/nature13318

Takayama, S., & Isogai, A. (2005). Self-incompatibility in plants. *Annual Review of Plant Biology*, *56*(1), 467-489. https://doi.org/10.1146/annurev.arplant.56.032604.144249

Tian, M., Yang, W., Zhang, J., Dang, H., Lu, X., Fu, C., & Miao, W. (2017). Nonsense-mediated mRNA decay in *Tetrahymena* is EJC independent and requires a protozoa-specific nuclease. *Nucleic Acids Research*, *45*(11), 6848-6863. https://doi.org/10.1093/nar/gkx256

Vekemans, X., & Castric, V. (2021). When the genetic architecture matters: evolutionary and ecological implications of self versus nonself recognition in plant self‐incompatibility. *New Phytologist*, *231*(4), 1304-1307. https://doi.org/10.1111/nph.17471

Wang, G., Chen, K., Zhang, J., Deng, S., Xiong, J., He, X., Fu, Y., & Miao, W. (2020). Drivers of Mating Type Composition in *Tetrahymena thermophila*. *Genome Biology and Evolution*, *12*(12), 2328-2343. https://doi.org/10.1093/gbe/evaa197

Wang, S., Gao, D., Penny, J., Krishna, S., & Takeyasu, K. (1997). P-Type ATPases in *Tetrahymena*. *Annals of the New York Academy of Sciences*, *834*(1), 158-160. https://doi.org/10.1111/j.1749-6632.1997.tb52247.x

Wang, S., & Takeyasu, K. (1997). Primary structure and evolution of the ATP-binding domains of the P-type ATPases in *Tetrahymena thermophila*. *American Journal of Physiology*, *272*(2 Pt 1), C715-728. https://doi.org/10.1152/ajpcell.1997.272.2.C715

Wolfe, J., & Feng, S. (1988). Concanavalin A receptor 'tipping' in *Tetrahymena* and its relationship to cell adhesion during conjugation. *Development*, *102*(4), 699. http://dev.biologists.org/content/102/4/699.abstract

Wolfe, J., & Grimes, G. W. (1979). Tip Transformation in *Tetrahymena*: A Morphogenetic Response to Interactions Between Mating Types. *The Journal of Protozoology*, *26*(1), 82-89. https://doi.org/10.1111/j.1550-7408.1979.tb02737.x

Wolfe, J., Pagliaro, L., & Fortune, H. (1986). Coordination of concanavalin-A-receptor distribution and surface differentiation in *Tetrahymena*. *Differentiation*, *31*(1), 1-9. https://doi.org/https://doi.org/10.1111/j.1432-0436.1986.tb00375.x

Wu, J., Wang, S., Gu, Y., Zhang, S., Publicover, S. J., & Franklin-Tong, V. E. (2011). Self-incompatibility in *Papaver rhoeas* activates nonspecific cation conductance permeable to Ca2+ and K+. *Plant Physiology*, *155*(2), 963-973. https://doi.org/10.1104/pp.110.161927

Xiong, J., Lu, X., Lu, Y., Zeng, H., Yuan, D., Feng, L., Chang, Y., Bowen, J., Gorovsky, M., Fu, C., & Miao, W. (2011). *Tetrahymena* Gene Expression Database (TGED): a resource of microarray data and co-expression analyses for *Tetrahymena*. *Sci China Life Sci*, *54*(1), 65-67. https://doi.org/10.1007/s11427-010-4114-1

Yan, G., Yang, W., Han, X., Chen, K., Xiong, J., Hamilton, E. P., Orias, E., & Miao, W. (2021). Evolution of the mating type gene pair and multiple sexes in *Tetrahymena*. *iScience*, *24*(1), 101950. https://doi.org/10.1016/j.isci.2020.101950

Figure legends

Figure 1. Mating-type recognition in *T. thermophila*. (**A**) Example of self and non-self mating-type recognition. When one cell of mating type I encounters another, costimulation and mating do not occur. When a cell of mating type I encounters a cell of another mating type (II–VII), the cells enter the costimulation stage and go on to form a pair. (**B**) Two typical phenotypes of the

544 costimulation stage are Tip transformation and Con-A receptor appearance. Yellow dashed circle,
545 transformed cell tip (center, single cell) or pairing junction (right, cell pair). Note that Tip
546 transformation may become less obvious after Con-A staining. (**C**) *MTA* and *MTB* gene structure
547 and MTA and MTB protein domain information (Cervantes et al., 2013). MTA and MTB form a
548 head-to-head gene pair. For each gene, the terminal exon is shared by all mating types and the
549 remainder is mating-type-specific (the sequence differs for each mating type). The mating-type-
550 specific region of each protein is predicted to be extracellular.

551 **Figure 2. Mating-type proteins are essential for mating-type recognition.** (**A**) Experimental
552 procedure for the costimulation experiments. Starved WT cells of mating types V (WT-V) and VII
553 (WT-VII) were separately pre-incubated with the indicated mating type VI mutant (9 : 1 ratio) for
554 30 min and then the pre-incubated cells were mixed at a 1 : 1 ratio. Note that before mixing the
555 costimulated cells, any potentially pairing cells were separated by shaking. (**B**) Effect of pre-
556 incubation with Δ*MTA* and Δ*MTB* on the rate of pair formation. Each experiment was repeated
557 three times, with > 100 pairs counted at each time point. Matched two-way ANOVA was used for
558 the statistical analysis. N.S., not significant; *, $P < 0.05$; **, $P < 0.01$; ***, $P < 0.001$; ****,
559 $P < 0.0001$. Unpaired mutants were excluded when calculating the pairing rate (see Materials
560 and Methods). (**C**) Tip transformation, a hallmark of costimulation. Costimulated cells from two
561 different WT strains are shown because their tips have slightly different shapes. Each strain was
562 pre-incubated with the strain shown in subscript. Yellow dashed circle, transformed cell tip. (**D**)
563 Appearance of Con-A receptors, another hallmark of costimulation. In all, ~90% cells show Con-A
564 receptor fluorescence (panels 4, 5 and 9). The low percentage of cells (7%) with fluorescence in

565 panel 7 were probably WT cells, which comprised 10% of the pre-incubation culture. Each strain
566 was pre-incubated with the strain shown in subscript. Yellow dashed circle, Con-A receptor
567 fluorescence.

568 **Figure 3. Proteins that interact with MTA and MTB.** (**A**) Construction of HA-tagged strains. All of
569 the tagged strains mated like WT cells. (**B**) Statistical analysis of IP-MS data. A total of 13
570 experiments were carried out. WT samples (untagged) were run in parallel for each sample. All
571 13 WT controls were combined as the background control. Red dot, high-confidence interaction;
572 dark gray dot, low-confidence interaction. Gene identifiers are summarized in Figure 3–Source
573 data 2. Note that the wash buffer contained 1% Triton X-100 and 600 mM NaCl. (**C**) Interaction
574 network based on IP-MS data. Orange oval, bait; blue oval, high-confidence prey; light gray dot,
575 low-confidence prey; black line, high-confidence interaction; dark gray dashed line, low-
576 confidence interaction; light gray dotted line, interaction supported by a few peptides (these
577 proteins were shown because their coding genes are coexpressed with *MTA* and *MTB* and
578 deleting them affects mating behavior). (**D**) Diagram of functional domain annotation of MTRC
579 components. GFR, growth factor receptor domain; PLF, pectin lyase fold; Poly-E, poly-glutamic
580 acid region; NTH, P-loop-containing nucleotide triphosphate hydrolase. (**E**) Expression profiles of
581 genes whose protein products were identified by IP-MS as potentially components of the MTRC.
582 Expression data is derived from *Tetra*FGD (Xiong et al., 2011).

583 **Figure 4. Mating-type proteins are cell surface proteins but do not localize to cilia.** (**A**)
584 Fractionation of *MTA7-HA* cells (please see Figure 4–figure supplement 1A for the experimental
585 process). Red arrowhead, MTA7-HA; F, flow through; P, pellet; R, resin; S, supernatant; W, wash.

586 The MTA signal is undetectable until S3 (enriched membrane proteins), and only appears after
587 affinity chromatography (R). (**B**) WB analysis of cell surface proteins. Red arrowhead, MTA7-HA;
588 M, marker; C, negative control (unbiotinylated). (**C**) Cilia isolation and purification. (**D**) WB
589 analysis of IP products of membrane and ciliary proteins. Mem, membrane; R, resin; S,
590 supernatant. The same amount of *MTA7-HA* cells was used for the membrane and ciliary protein
591 IPs. The full blot is shown in Figure 4–figure supplement 1B. (**E**) Construction scheme for eGFP-
592 tagged MTB2 strains. (**F**) Costimulated MTB2-eGFP cell. (**G**) Paired MTB2-eGFP cell. To induce
593 MTB2-eGFP overexpression, cells were treated with 10 ng/ml Cd^{2+} for 5 h. Green, eGFP signal;
594 red, tubulin signal; yellow dashed line, cell outline. The focal plane of these images is the cell
595 surface.

596 **Figure 5. Stimulation experiments using MTAxc and/or MTBxc.** (**A**) WT cells were treated with
597 MTAxc and/or MTBxc proteins (30 pg/ml, 1 h) of different mating-type specificities. WT-VI cells
598 were treated with MTA/B7xc protein, and WT-VII cells were treated with MTA/B6xc protein.
599 Treated cells were washed twice before mixing to remove residual proteins from the starvation
600 medium. Note that the starvation medium used for washing had been previously used for cell
601 starvation because *T. thermophila* cells secrete mating-essential factors during starvation (Adair
602 et al., 1978). Each experiment was repeated five times. (**B, C**) The percentages of cells paired at
603 60 min (**B**) and 75 min (**C**) were used for the statistical analysis (method described in Figure 2B).
604 (**D**) WT cells (mating types VI and VII) were treated with MTAxc and/or MTBxc proteins of the
605 same mating-type specificity (as described in (**A**)). (**E, F**) The percentages of cells paired at 75 min
606 (**E**) and 240 min (**F**) were used for the statistical analysis (method described in Figure 2B).

607 **Figure 6. Results of treatment with either MTAxc or MTBxc proteins.** (**A**–**F**) Dose–response
608 effect of treatment with MTA6xc or MTB6xc protein. (**A**–**C**) MTA6xc results. (**D**–**F**) MTB6xc
609 results. Cells of mating types I and VII were used for these experiments. Experimental and
610 statistical methods were as described for Figure 5, except for protein concentrations. (**G**–**J**)
611 MTA6xc or MTB6xc proteins affect the mating of various combinations of other WT mating types.
612 (**G**) MTA6xc results. Both mating partners were treated. (**H**) MTB6xc results. Both mating
613 partners were treated. (**I**) MTA6xc results. Cells of only one mating type were treated. Note that
614 mating type VI cells were used in these experiments. (**J**) MTB6xc results. Note that mating type VI
615 cells were used in these experiments. Experimental and statistical methods were as described for
616 Figure 5. Red superscript "T" in (**I**) and (**J**) indicate the strain treated with MTA6xc or MTB6xc.
617 The mating types used in each experiment is shown in the top-left corner.

618 ## Supplementary Information

619 **Figure 1 – figure supplement 1. *T. thermophila* lifecycle.** *T. thermophila* has seven mating types.
620 Cells divide asexually when nutrition is adequate. After starvation, cells of any two different
621 mating types recognize each other and enter a pre-conjugation stage called costimulation. In this
622 stage, cells first become round (Fujishima et al., 1993); subsequently, their cell tips are
623 transformed into a curved shape (Wolfe & Grimes, 1979) and the Con-A receptor becomes
624 detectable (Wolfe & Feng, 1988; Wolfe et al., 1986). Costimulated cells then form pairs via a
625 rotating behavior (Video S1, S2). During the sexual life cycle (conjugation), cells undergo a series
626 of sexual events such as meiosis and reciprocal fertilization (for details refer to (Orias et al.,
627 2011)). Exconjugants (separated pairs) finally form parent-like progeny when nutrition becomes

628 available, but remain sexually immature. After ~60 fissions, cells mature and their mating type is
629 determined and becomes fixed (for details of mating-type determination, refer to (Cervantes et
630 al., 2013; Lin & Yao, 2020; Orias et al., 2017)).

631 **Figure 2 – figure supplement 1. Mating-type gene deletion strains do not costimulate WT cells.**
632 (**A**) Pre-incubation results predicted by a simple receptor–ligand model of mating-type
633 recognition, in which one mating-type protein is designed ligand (L) and the other receptor (R).
634 The type of cell used to costimulate is shown on the left. The expected result of costimulation if
635 *T. thermophila* were to use non-self mating-type recognition (1, 3, 5) or self mating-type
636 recognition (2, 4, 6). If this simple model were true, deleting the receptor would have a different
637 effect on costimulation to deleting the ligand. However, the experimental results showed that
638 neither Δ*MTA* nor Δ*MTB* can fully transmit/receive mating signal to/from WT cells. Therefore,
639 mating-type recognition in *T. thermophila* does not occur via the simple receptor–ligand binding
640 mechanism. Costim, costimulation. (**B**) Pre-incubation with Δ*MTA* or Δ*MTB* does not influence
641 the pairing rate. The experimental method was as described in Figure 2A except that the pre-
642 incubation time was 16 h.

643 **Figure 4 – figure supplement 1. Cell fractionation MTA7-HA cells.** (**A**) Experimental process for
644 cell fractionation. (**B**) Affinity purification results of the soluble pool (S2, shown in panel A) and
645 ciliary protein. C+, positive control (i.e., IP product of MTA7-HA cell membrane); R, resin; S,
646 supernatant. No MTA7-HA signal was detected in the soluble pool or in ciliary protein samples,
647 even after affinity purification.

Figure 4 – figure supplement 2. Confocal images of ciliary sections and cell interior sections of MTB2-eGFP cells. (**A**) No MTB2-eGFP signal was associated with cilia. (**B**) In the cell interior section, MTB2-eGFP protein was detected on the plasma membrane and in intracellular structures, probably the ER and Golgi.

Figure 5 – figure supplement 1. Expression and purification of extracellular regions of mating-type proteins. (**A**) Schematic diagram showing truncated and full-sized proteins. (**B**–**E**) Size-exclusion chromatography for MTA6xc (**B**), MTB6xc (**C**), MTA7xc (**D**), and MTB7xc (**E**). Left, elution profile; right, Coomassie blue staining. In, input; M, marker.

Figure 5 – figure supplement 2. Treatment with MTA6xc and/or MTB6xc proteins fails to induce costimulation. (**A**) Tip transformation. Yellow dashed circle, transformed cell tip. (**B**) Con-A receptor appearance. Yellow dashed circle, Con-A signal. Cells of mating type VII were used for these experiments.

Video 1. Mating behavior of *T. thermophila*.

Video 2. Mating behavior of *T. thermophila*. To distinguish cells of different mating types, smaller mating type VI cells and larger mating type VII cells were used in this experiment.

Video 3. Cells of different mating types form a pair, whereas cells of the same mating type become separated after a short contact. To distinguish cells of different mating types, smaller mating type VI cells and larger mating type VII cells were used in this experiment.

Figure 3–Source data 1. IP-MS results.

Figure 3–Source data 2. Gene identifiers.

Figure 4–Source data 1. MS analysis of MTA7-HA cilia protein.

669 **Figure 4–Source data 2. MS analysis of MTB2-eGFP cilia protein.**

670 **Appendix 1—table 1. Strains used in this study.**

671 **Appendix 1—table 2. Primers used in this study.**

Figure 1

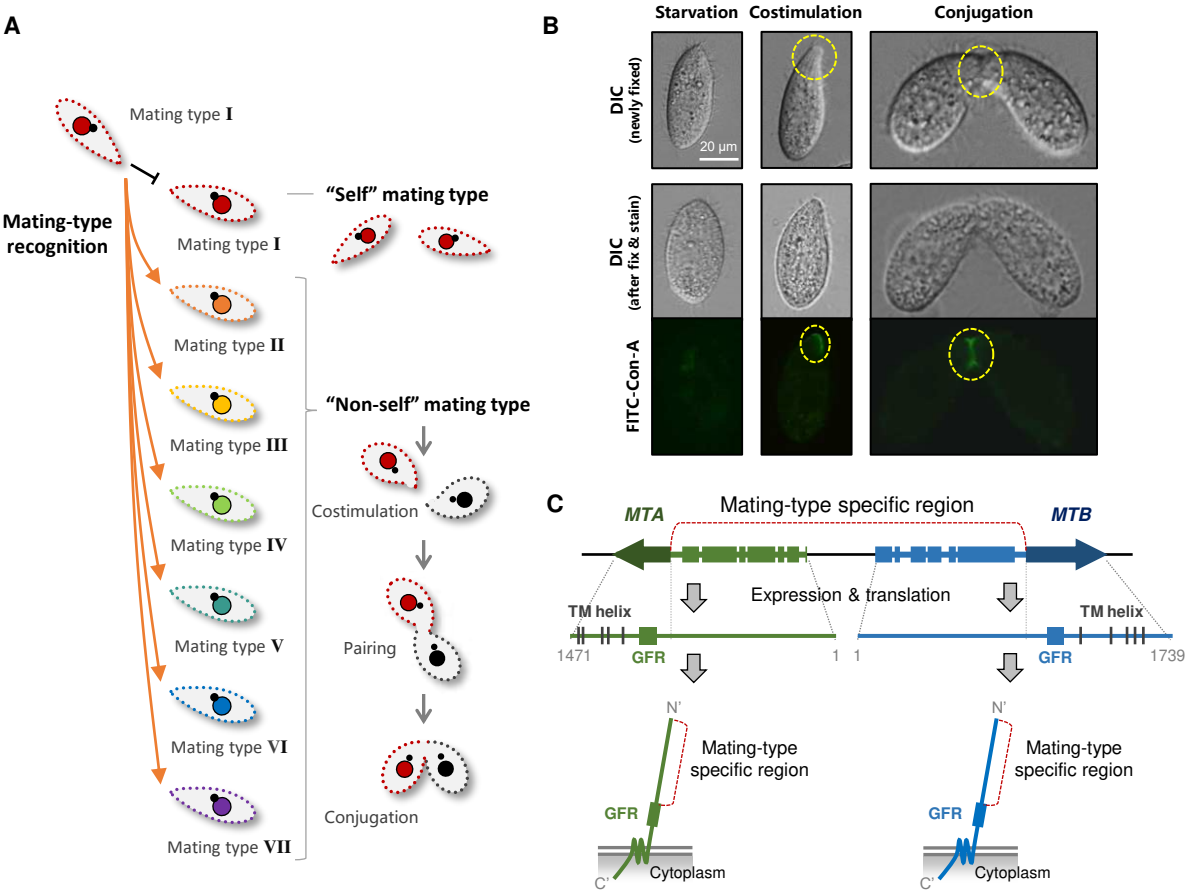
A
Mating type I
Mating-type recognition
Mating type I
"Self" mating type
Mating type II
Mating type III
Mating type IV
Mating type V
Mating type VI
Mating type VII
"Non-self" mating type
Costimulation
Pairing
Conjugation
B
Starvation
Costimulation
Conjugation
DIC (newly fixed)
20 μm
DIC (after fix & stain)
FITC-Con-A
C
MTA
Mating-type specific region
MTB
Expression & translation
TM helix
1471
GFR
1
1
GFR
TM helix
1739
N'
Mating-type specific region
GFR
Cytoplasm
C'
N'
Mating-type specific region
GFR
Cytoplasm
C'

Figure 2

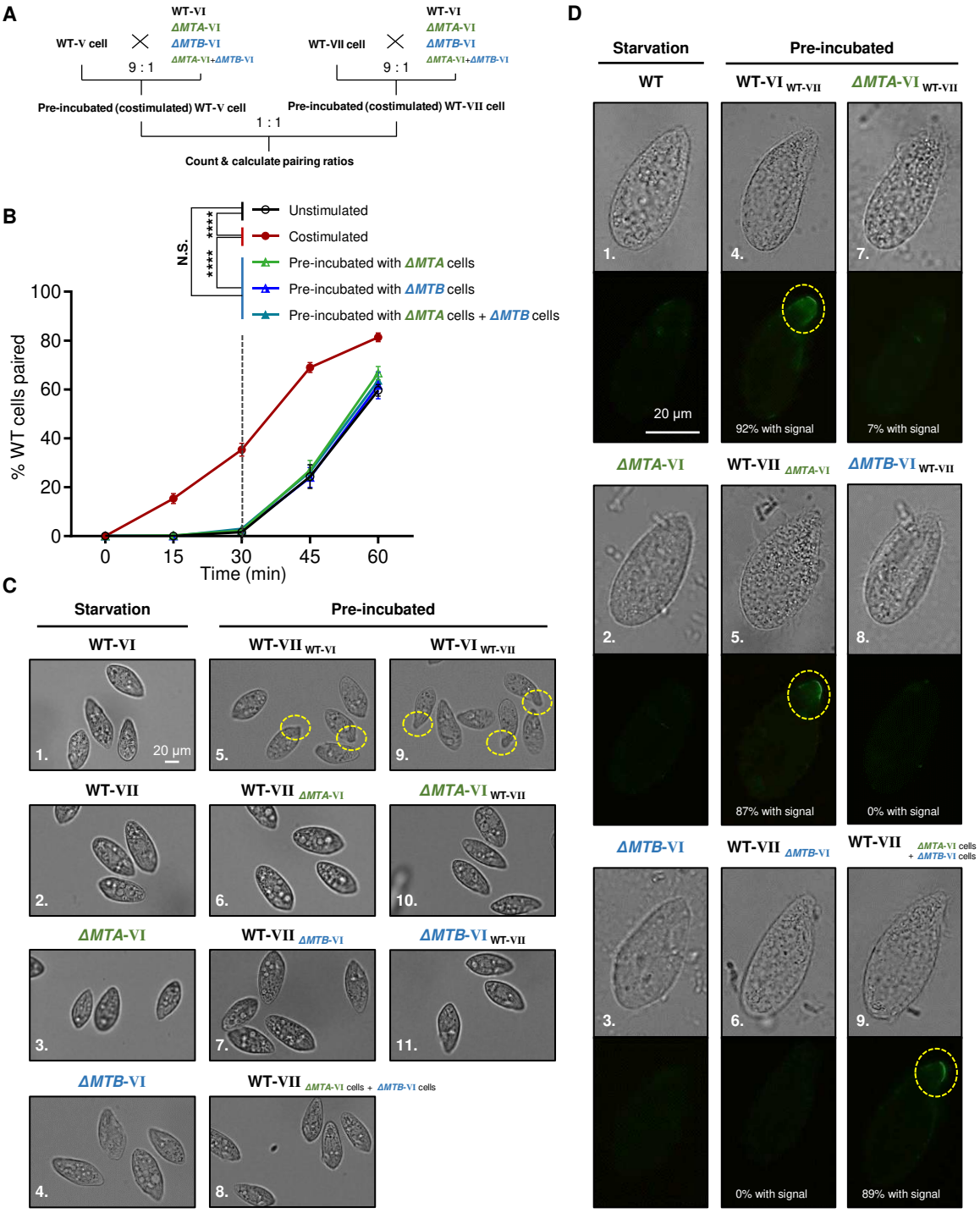
A
WT-V cell
WT-VI
ΔMTA-VI
ΔMTB-VI
ΔMTA-VI+ΔMTB-VI
9 : 1
WT-VII cell
WT-VI
ΔMTA-VI
ΔMTB-VI
ΔMTA-VI+ΔMTB-VI
9 : 1
Pre-incubated (costimulated) WT-V cell
Pre-incubated (costimulated) WT-VII cell
1 : 1
Count & calculate pairing ratios
B
Unstimulated
Costimulated
Pre-incubated with ΔMTA cells
Pre-incubated with ΔMTB cells
Pre-incubated with ΔMTA cells + ΔMTB cells
N.S.
****
****
% WT cells paired
100
80
60
40
20
0
0
15
30
45
60
Time (min)
C
Starvation
Pre-incubated
WT-VI
WT-VII WT-VI
WT-VI WT-VII
1.
20 μm
5.
9.
WT-VII
WT-VII ΔMTA-VI
ΔMTA-VI WT-VII
2.
6.
10.
ΔMTA-VI
WT-VII ΔMTB-VI
ΔMTB-VI WT-VII
3.
7.
11.
ΔMTB-VI
WT-VII ΔMTA-VI cells + ΔMTB-VI cells
4.
8.
D
Starvation
Pre-incubated
WT
WT-VI WT-VII
ΔMTA-VI WT-VII
1.
4.
7.
20 μm
92% with signal
7% with signal
ΔMTA-VI
WT-VII ΔMTA-VI
ΔMTB-VI WT-VII
2.
5.
8.
87% with signal
0% with signal
ΔMTB-VI
WT-VII ΔMTB-VI
WT-VII ΔMTA-VI cells + ΔMTB-VI cells
3.
6.
9.
0% with signal
89% with signal

Figure 3

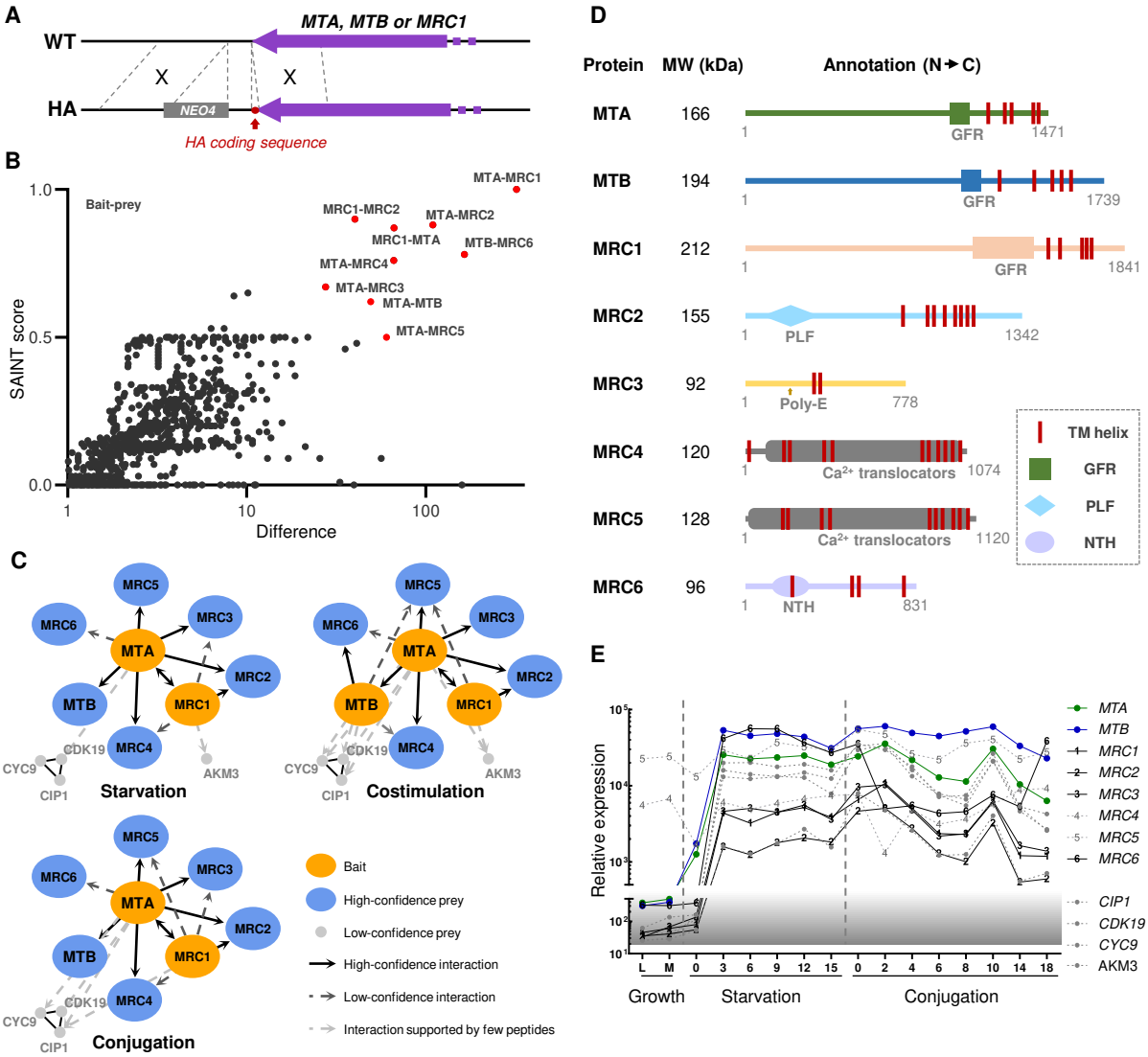
A
MTA, MTB or MRC1
WT
HA
NEO4
HA coding sequence
B
Bait-prey
SAINT score
Difference
MTA-MRC1
MRC1-MRC2
MTA-MRC2
MRC1-MTA
MTB-MRC6
MTA-MRC4
MTA-MRC3
MTA-MTB
MTA-MRC5
C
Starvation
Costimulation
Conjugation
Bait
High-confidence prey
Low-confidence prey
High-confidence interaction
Low-confidence interaction
Interaction supported by few peptides
D
Protein
MW (kDa)
Annotation (N→C)
MTA 166
MTB 194
MRC1 212
MRC2 155
MRC3 92
MRC4 120
MRC5 128
MRC6 96
GFR
PLF
Poly-E
Ca2+ translocators
NTH
TM helix
E
Relative expression
MTA
MTB
MRC1
MRC2
MRC3
MRC4
MRC5
MRC6
CIP1
CDK19
CYC9
AKM3
Growth
Starvation
Conjugation

Figure 4

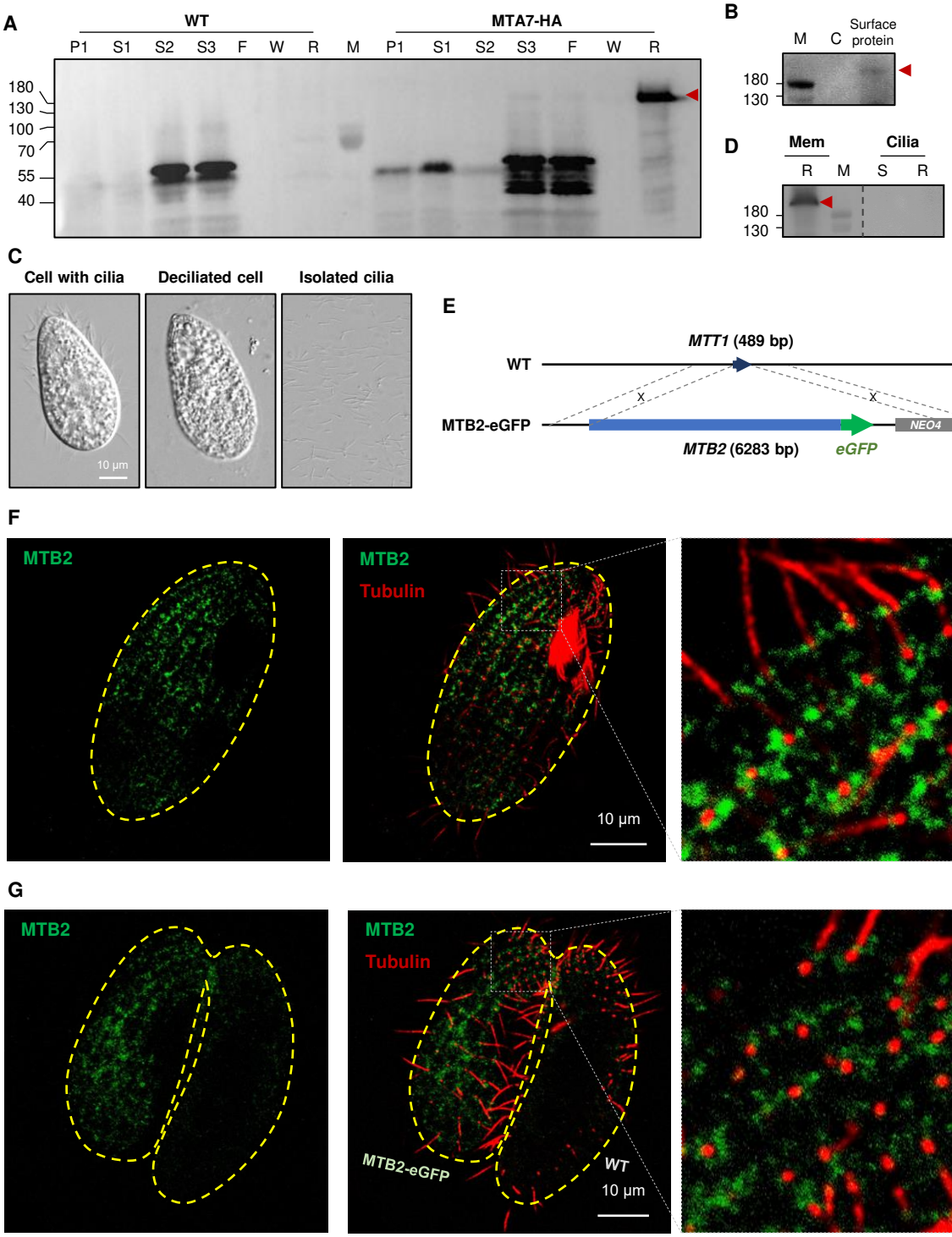
A
WT
MTA7-HA
P1 S1 S2 S3 F W R M P1 S1 S2 S3 F W R
180
130
100
70
55
40
B
M C Surface protein
180
130
D
Mem
Cilia
R M S R
180
130
C
Cell with cilia
Deciliated cell
Isolated cilia
10 µm
E
MTT1 (489 bp)
WT
MTB2-eGFP
NEO4
MTB2 (6283 bp)
eGFP
F
MTB2
MTB2
Tubulin
10 µm
G
MTB2
MTB2
Tubulin
MTB2-eGFP
WT
10 µm

Figure 5

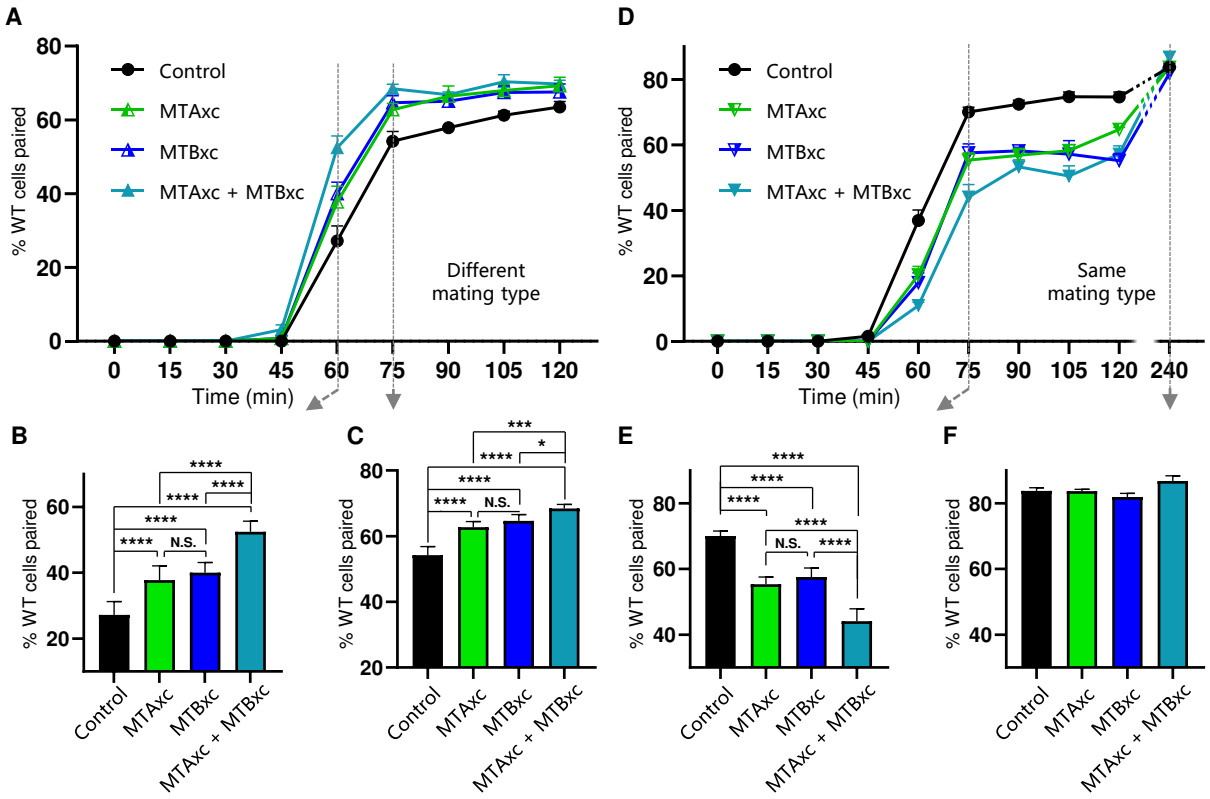
A
% WT cells paired
Control
MTAxc
MTBxc
MTAxc + MTBxc
Different mating type
Time (min)
D
Same mating type
B
C
E
F
N.S.
Control
MTAxc
MTBxc
MTAxc + MTBxc

Figure 6

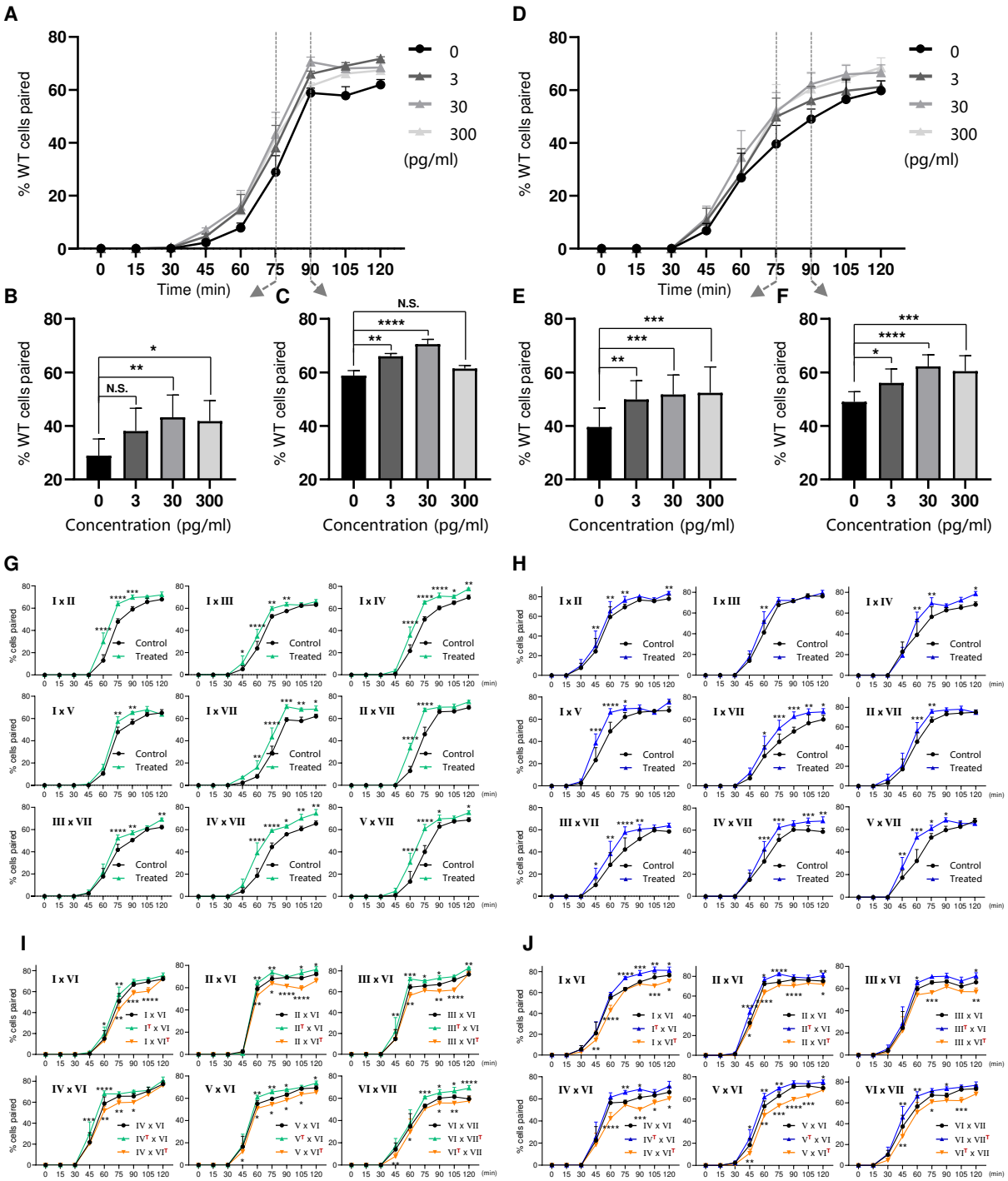
A
D
% WT cells paired
Time (min)
0
3
30
300
(pg/ml)
B
C
E
F
N.S.
Concentration (pg/ml)
G
H
I
J
% cells paired
Control
Treated
I x II
I x III
I x IV
I x V
I x VII
II x VII
III x VII
IV x VII
V x VII
I x VI
II x VI
III x VI
IV x VI
V x VI
VI x VII
(min)

Figure 1 – figure supplement 1

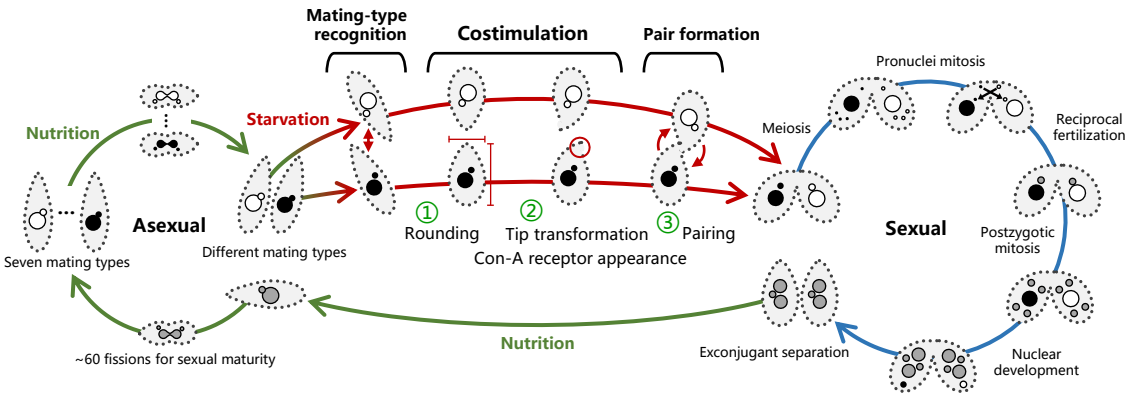

Figure 2 – figure supplement 1

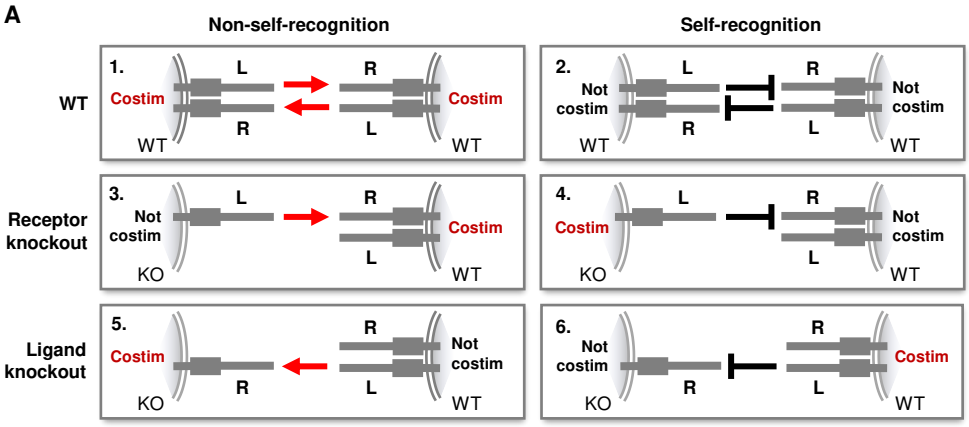

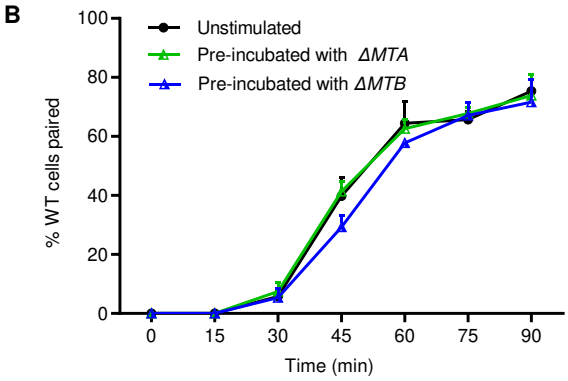

Figure 4 – figure supplement 1

A

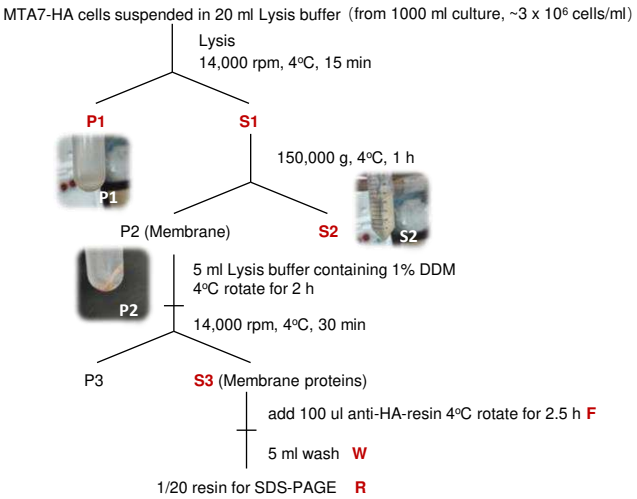

B

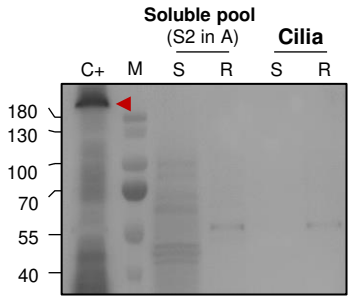

Figure 4 – figure supplement 2

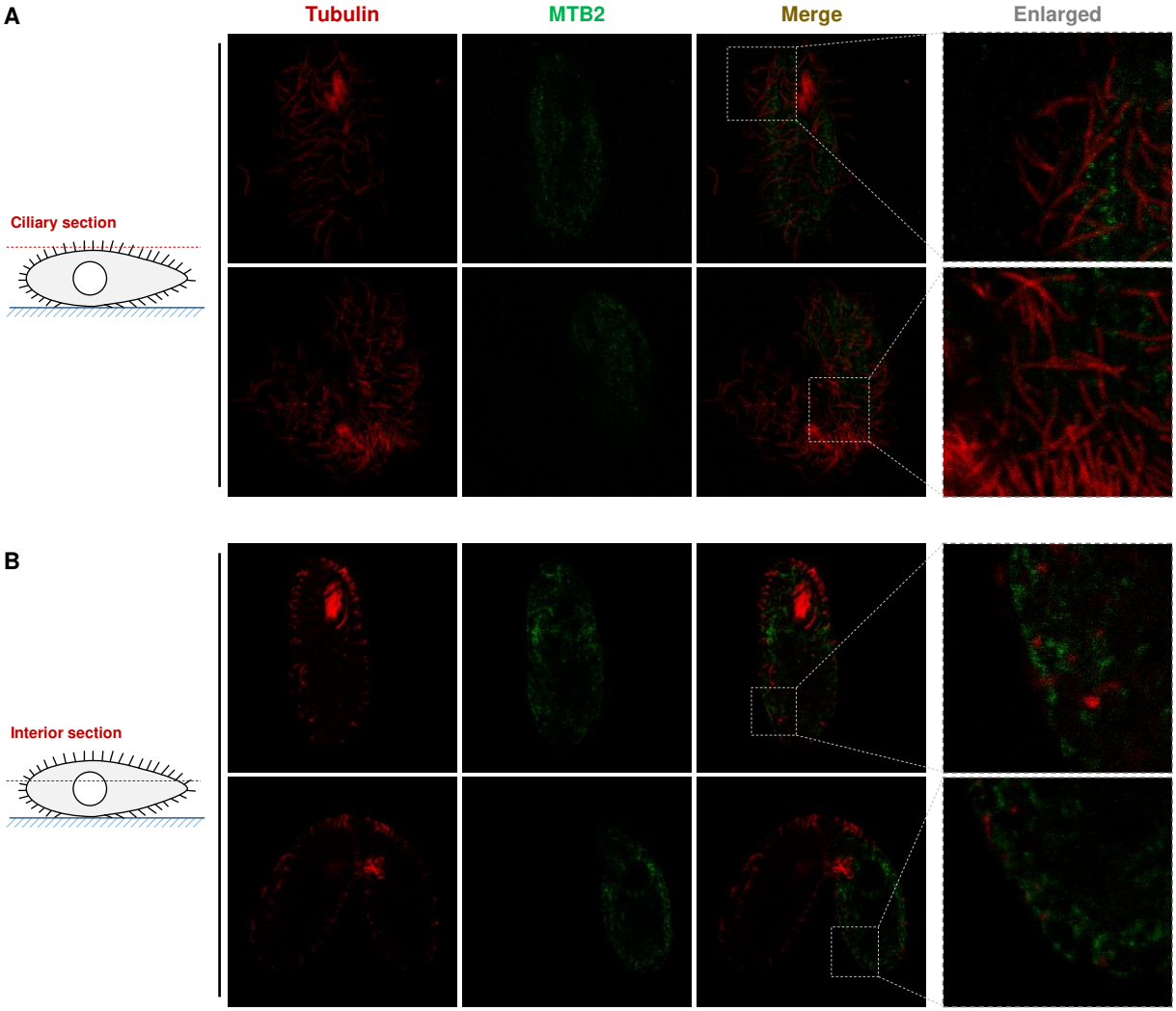

Figure 5 – figure supplement 1

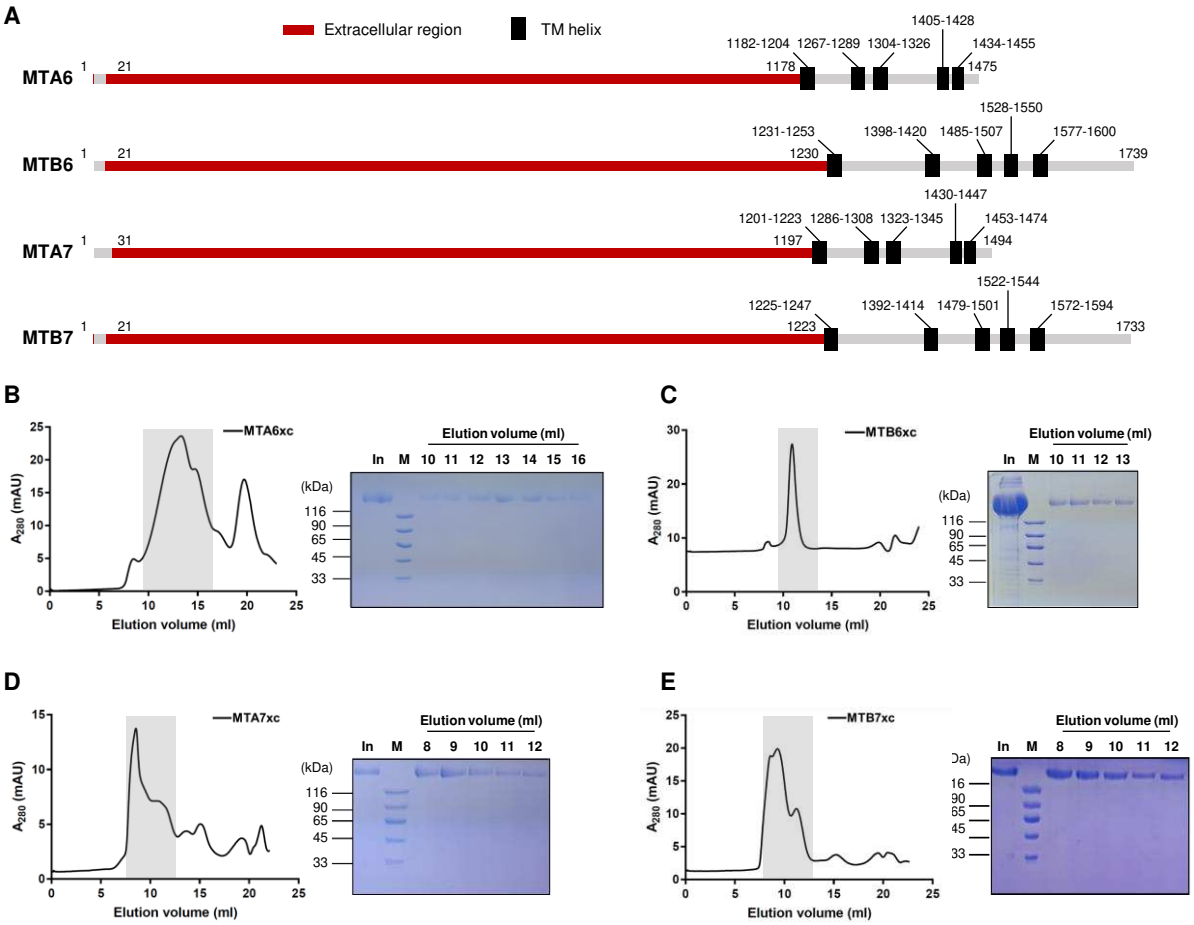

Figure 5 – figure supplement 2